



Original research article

Computer vision based train rolling stock examination

P.V.V. Kishore ^{*}, Ch. Raghava Prasad

Dept. of ECE, K L University, Green Fields, Vaddeswaram, Guntur, Andhra Pradesh, India

ARTICLE INFO

Article history:

Received 26 July 2016

Received in revised form 8 October 2016

Accepted 21 December 2016

Keywords:

High speed video analysis
 Intelligent rolling stock examination
 Shape prior models
 Shape invariant level sets
 Train bogie defect segmentation

ABSTRACT

Train Rolling stock examination involves visual observation of the moving train around 30Kmph to find defective bogie parts. A train coach moves on a couple of bogies consisting of wheels, suspension and other binding hardware. The health of the bogie decides the safety of the train. Railway personnel perform the rolling stock examination manually raising questions on reliability. Here we propose to use computer vision algorithms for extraction and localizing defective bogie parts from working parts. A wide-angle high-speed camera captures the moving train without motion artefacts. The objective is to use a single shape prior to power the level set function for object segmentation. Here we show the bogie part segmentation with one shape prior model for the entire length of the train. Experimentation on similar train bogies under different lighting tests the robustness of the level set functional with single shape prior. The proposed algorithm handles topological spatial deformations of the bogie parts in the video effectively. Segmenting defective parts with non-defective shape priors makes the algorithm independent of defect localization in the bogie part. This novel idea of computer vision based rolling stock examination using high-speed video can lessen human errors and aid in developing a crewless rolling stock examination. Further, the proposed work can be extended for early detection and prevention of rail accidents due to transit part failures.

© 2016 Elsevier GmbH. All rights reserved.

1. Introduction

According to India Risk Survey 2012, around 15% of the industrial accidents happen in India and 90% of them are due to human errors and lack of proper maintenance of rolling stock. Here “Rolling Stock” is defined as moving machines with wheels, suspension, baring, etc. available on trains, which are designed for specific purpose. Engineering industry has contributed significantly in the economic growth of India. More than 17 lakh people are employed in this sector. The rate of fatal accidents amongst industrial workers is showing an upward trend. Most of the industrial accidents are caused by

- (a) Contact with exposed moving mechanical parts
- (b) Flying Parts
- (c) Fire
- (d) Human Errors

^{*} Corresponding author.E-mail addresses: pvvkishore@kluniversity.in, pvvkishore@gmail.com (P.V.V. Kishore), chrp@kluniversity.in (Ch.R. Prasad).

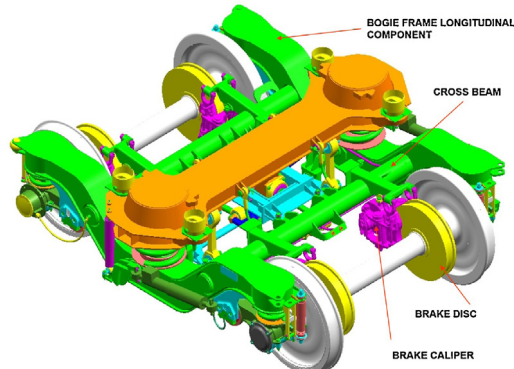


Fig. 1. Under carriage of a train called as FIAT Bogie and its parts from Indian Railway Manual.

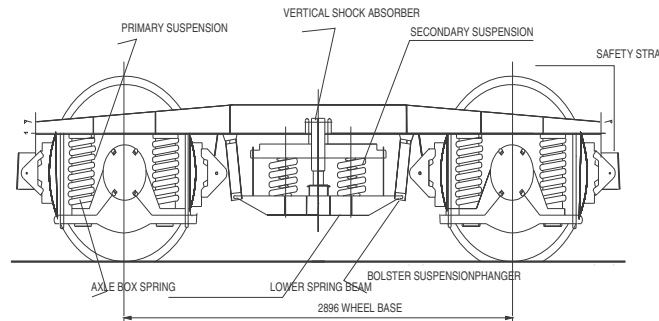


Fig. 2. Under carriage of a train called as ICF Bogie and its parts from Indian Railway Manual.



Fig. 3. Manned Rolling examination with two personal on either side of the moving train near a railway station.

The field of computer vision and its applications had made inroads into every field of engineering and sciences. One such novel application is being formulated in this work for monitoring train rolling stock. The moving and rolling portions of a train are called rolling stock. Rolling examination is vital for passenger trains to identify defects that are generated during movement of trains at high speeds. This process has ensured train safety for many decades now.

Railway safety is one of the primary responsibilities of all the rail operating companies around the globe from the invention of railroads two centuries ago [1]. With the development of computer technology in the recent decades, most of the safety systems in the world have become computer controlled. Two such systems are airways and seaways which have become fully automated by adapting computerization. Railroads are not far behind. In this framework, a number of methods have been proposed to monitor rails and rolling stock using computer vision [2,3]. Fig. 1 shows the under carriage of a train called as bogie. A rail coach sits on two of these bogies. Fig. 1 shows a model of a bogie called Fabrica Italina de Automobil Torino (FIAT). There are around six models operational in Indian railways. Fig. 2 shows another model called ICF model which is a part of 70% of Indian trains.

Actually, the train moves on a set of two bogies shown in Figs. 1 and 2. Failure of the bogie during transit questions the safety record of the railway organizations. To ensure safety of the train passengers, railways employ a process called rolling stock examination (RSE). Examination involves trained vision and auditory human senses to identify defects through observation of moving train. The train during observation is moving at around 30kmph. The process followed by railway operators in most of the Asian countries is pictured in Fig. 3.



Fig. 4. Rolling examination with high speed sports action camera for video database creation.

The results of the examination are a data sheet (office spread sheet) with defects and their intensities at various locations. This information is passed to the following station maintenance staff to attend the problem.

Two personal for monitoring and a third person for noting the defects on either ends of the station make up a total team of 6 personal per train for examination. The following are the drawbacks identified: in the manned process

- Human indulgence – error prone detection.
- Personal work load increases at peak hours – bound to make mistakes.
- Critical defects attended by maintenance staff in next station.
- Weather dependent system.
- Commercially a Lossy system.

This paper proposes a novel application of computer vision and machine learning algorithms to rolling stock examination. Fig. 4 shows our team members collecting video database of rolling stock alongside rolling examination team of Indian railways.

2. Related Work

Few researchers in literature have actually attempted work related to railway computer vision and processing. Machine vision is assisting automobile [4], transportation [5], structural [6], agricultural [7] and manufacturing [8] industry for around two decades now. Specialized cameras such as high speed, hyperspectral and laser cameras are used for video capture in industries. Bottling plants around the world use high-speed action cameras that record at 5000 frames per second to separate defective bottles from good ones when they are travelling on a conveyor at 85KMPH.

Rail industries around the world are relatively slow in adapting computer vision for maintenance tasks. Rolling examination is prevalent for every passenger train in Indian subcontinent to prevent accidents due to bogie parts failure in transit. The idea is to replace humans for this task with high-speed cameras and an algorithm to identify defects. The real challenge in designing solutions that achieve good performance with respect to imposing constraints by the complexity of the problem gives research motivation.

Fuzzy weighted logarithmic least squares method is studied for train rolling stock examination with machine vision. Video acquired with normal camera at 30fps of the rolling stock is thresholded and a fuzzy model based on the triangular fuzzy number (TFN) is built. Weighted logarithmic least square method classifies the segmented rolling parts. The model evaluation process described in [9] does not comment on the accuracy of detection and performance of the algorithm under various natural circumstances.

Embedded system based intelligent monitoring of rolling stock for safety enhancement in rail transit is a constrained solution proposed in [10]. This work reviews models for rolling stock failure with observable parameters for failure during movement of trains in real time. Artificial immune algorithm makes a detection and prediction of health of rolling stock on the data collected from a set of sensors attached to the rolling stock. But signal noise from the sensors in transit is a major issue.

Most of the industrial safety in the current scenario is based on cost cutting maintenance. In this regard, the motive of the authors in [11] deals with preventive maintenance (PM) forecasting to decrease the budget distribution for rolling stock examination. The authors use heuristic search algorithms such as genetic algorithm and simulated annealing to discover optimal maintenance breaks for rolling stock life span maximization. Extensions are added to calculate optimum number of spares required during maintenance cycles and their market availability in the long run. Automation of the entire process is a void that could have changed the course of rolling stock maintenance.

Developers in [12] worked on wireless monitoring of rolling stock with extensive reviews and analysis which leads towards potentially equivalent advantages of the prior model. The authors propose a standardized framework for rolling examination with a multi-hop mesh network. The network provides temporary and semi-permanent observable functions of rolling stock by localized network processing along with energy harvesting power management through wireless capability.

Accordingly, the methods complement each other well for the job, except that they could not capture the entire essence of rolling stock examination.

In the recent past researchers focused on thickness measurement of lining-type brake with computer vision for automatic rolling stock monitoring. To spot the round outline of the disk lining brake, interest points are detected with Hough transform and the brake edge is explored for anomalies in the region of interest. The paper also gives a mechanism to test the algorithm in real time by setting up cameras on tracks under the moving bogies. Experimental testing of the proposed system measures the thickness of lining-type brake with a precision of 1.15 mm, at the distance of 1.0 m from the camera [13]. Similar methods and systems are being executed for break and wheel systems of bogies [14,15] using computer vision and pattern classification for extracting and clustering brake shoe defects with a real time on track installed high speed camera.

Experimental module Technicatome has been developed as a demonstrator for RATP (the Paris subway company) based on interconnected digital systems is reported in [16]. This demonstrator is currently in operation on an MF 88 train set to the long existing and still operated with conventional relay-based systems.

This paper proposes to improve on the proposed methods by installing a high speed camera on the side of the track for rolling stock examination. The proposed methods are few and their reliability is questionable as they fail to represent of the rolling stock examination. From the Indian railway manual [1], there are around 10 important and crucial things to be checked during rolling examination. Some of them are, part breakages, hanging parts, dragging parts, pushing parts, missing screws, brake linings, suspensions, holding pins, axel boxes on wheels, wheel movement on rails and finally flat tire etc. Through this work we simulated bogie part extraction and defect identification from high speed video of moving trains.

Segmentation of the captured high speed bogie video gives a 2D view of each rolling stock component. The main contributions of our method are:

- (i) We propose a new approach for focused object extraction from a densely packed similar characteristic object background using weighted shape prior active contours.
- (ii) The movement of train induces deformation in shape, orientation and location to the bogie parts because of fixed camera angle. The proposed level set handles these deformation with a single shape prior model per part.
- (iii) Single shape prior model with shape invariance takes care of cluttered and hidden parts on the transit train.
- (iv) Segmenting defective parts with Non-defective shape priors by weigh vector adjustment is attempted successfully in this work.

The flow in the rest of the paper is: Weighted shape priors with active contours are presented in section 3. Section 4 gives results of the experiments with various train models and defects. Related outcomes with conclusions are embraced in Section 5.

3. Shape prior level sets

The level set functional introduced by Osher [17] is the most widely applied level set for image and video segmentation. Multiple models used this approach: edge consistency by Malladi [18] and Caselles [19], constant intensity without edges by Chan [20], texture information by Brox [21] and motion information by Cremers [22].



Fig. 5. Rolling examination with high speed sports action camera for video database creation.

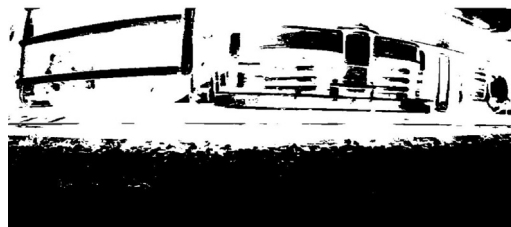


Fig. 6. Rolling examination CV active contour model on a high speed video frame at 1745th iteration for full HD frame 1080p.

Shape priors provide additional information into the formation of level set functional. Local spatially independent statistical shape model [23] and global deformation model [24] are two popular approaches under this class. Object segmentation and tracking use [25] level sets with dynamical shape priors by placing the initial contour near to the object regions. The material also gives insights into using multiple contemplating shape priors to extract several objects in an image sequence.

Statistical Gaussian shape models [25] does not go down well with level set formulation as the most of the real world objects does not fit into Gaussian models. Shapes are represented by signed distance function which occupy a nonlinear space. Another important issue is shape invariance where a deformed object tries to match the shape model [26–28]. Proposed iterative optimization such as gradient descent to propel the contour using object transformations till it aligns with the object of interest. The number of extra iterations needed for correct alignment and the stopping criteria for gradient descent are not mentioned in this work. Segmentation results are good for single object with simple backgrounds, but limits performance for objects under complex backgrounds.

To get a feel of the difficulty in object extraction in a rolling stock frame, we present a frame of rolling stock high-speed video in Fig. 5.

Carefully gauging Fig. 5 for part extraction and defect identification is a complicated task even with shape prior models based on color, texture and statistical shape information. We developed our variational model from [25] by introducing shape invariance of the shape prior. Here the level set functional evolves not in the higher image dimension but in the lower subspace of the object shape prior. Such a solution is independent of local estimates of shape parameters, which are otherwise updated iteratively after every deformation. This method shows invariance to certain types of transformations. The prospects of using color and texture propelled level sets for rolling frame, shown in Fig. 5, are difficult due the narrow color and texture variations between rolling pixels.

The level set model introduced by [19] and few others is an image segmentation model based on a closed contour spreading in the image plane adhering to object edges. An implicitly defined contour of arbitrary shape Θ in the image plane $O : \{o(x, y) \subset \mathbb{R}^2\}$ as the zero level set of an embedding function $\phi : O \rightarrow \mathbb{R}$:

$$\Theta = \{x, y \in O \mid \phi(x, y) = 0\} \quad (1)$$

Level set function ϕ evolves instead of contour Θ itself giving advantages in the form of no marker control and immune to topological deformations of the active contour in the image plane. Here we focus on Chan Vese (CV) level set functional formulated from [20] in the image plane $I : \Theta \rightarrow \mathbb{R}^+$ as

$$E^{CV}(\phi) = \int_{\Theta} (I(x) - C^+)^2 H(\phi(x)) dx + \int_{\Theta} (I(x) - C^-)^2 (1 - H(\phi(x))) dx + \lambda \int_{\Theta} |\nabla H\phi(x)| dx \quad (2)$$

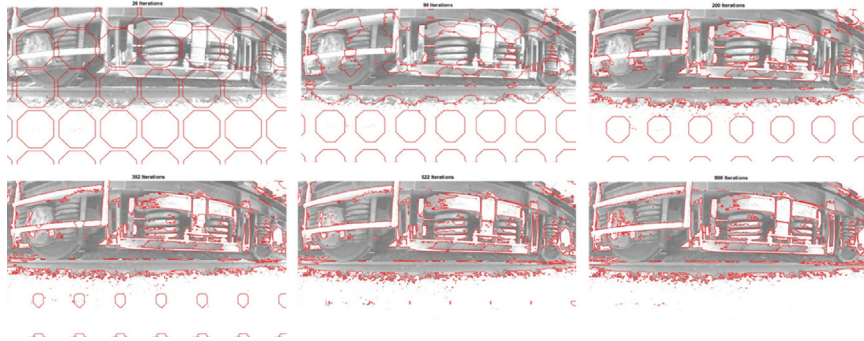


Fig. 7. Rolling examination CV active contour model with modified smoothing function on a high speed video frame with increasing order of iterations from 1 to 900.

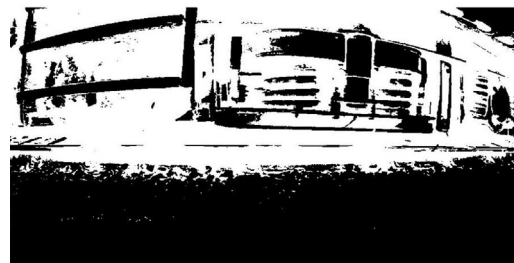


Fig. 8. Final Bogie Segment with modified smoothing term in CV active contour model at 900th iteration.

$I(x, y)$ is a 2D image plane represented as $sl(x)$. Here $H(\phi(x))$ is a Heaviside step function. C^+ represents average intensity of pixels considered constant in positive ϕ region and C^- represents negative ϕ region constant. The last term in the Eq. (2) tries to keep a smoothing contour during evolution and λ is proportionality constant deciding on the minimum amount of separation needed between boundaries. The first two parts constitute external energy representing error between the image and piecewise constant approximations of the evolving level set functional. Gradient descent minimization of the level set ϕ gives a curve evolution expression

$$\frac{\partial \phi}{\partial t} = -\frac{\partial E^{CV}}{\partial \phi} = \delta(\phi) \left[\lambda \left(\nabla \cdot \left(\frac{\nabla \phi}{|\nabla \phi|} \right) \right) - (I(x) - C^+)^2 + (I(x) - C^-)^2 \right] \quad (3)$$

CV model proposed the $\delta(\phi)$ term which helps level set detect even the internal edges. Applying this level set model in (3) to segment rolling parts for part segmentation as shown in Fig. 6 for a video frame shown in Fig. 5.

The purpose of rolling stock examination with computer vision is to separate bogie parts for monitoring its health. This enables whether to move the train further by repairing the part or by replacing it. The final segmented output from the CV model is in Fig. 6. Few parts are missing and remaining are under segmented or over segmented making it difficult to draw boundaries between them and represent their shape features. We have in our previous work remodeled the smoothing term in CV using morphological differential gradient. The first term in Eq. (3), $\left(\nabla \cdot \left(\frac{\nabla \phi}{|\nabla \phi|} \right) \right)$ is remodeled as $\left\{ (\nabla^{dia}) \cdot \frac{\nabla^{dia} \phi}{|\nabla^{dia} \phi|} - (\nabla^{ero}) \cdot \frac{\nabla^{ero} \phi}{|\nabla^{ero} \phi|} \right\}$, where ∇^{dia} and ∇^{ero} morphological gradient operator for dilation is and for erosion. The adapted expression for curve evolution is

$$\frac{\partial \phi}{\partial t} = -\frac{\partial E^{CV}}{\partial \phi} = \delta(\phi) \left[\lambda \left(\left\{ (\nabla^{dia}) \cdot \frac{\nabla^{dia} \phi}{|\nabla^{dia} \phi|} - (\nabla^{ero}) \cdot \frac{\nabla^{ero} \phi}{|\nabla^{ero} \phi|} \right\} \right) - (I(x) - C^+)^2 + (I(x) - C^-)^2 \right] \quad (4)$$

Fig. 7 shows the evolving level sets with the final segment at 900th iteration. The adjustment has improved the segmented image by cutting the number of iterations to around 44% over CV level set model. We also used it for improving the noise performance of ultrasound medical images in our latest publication [29].

Fig. 8 is the segmented frame from 900th level set of modified CV model. Comparing visually Fig. 7 and 8, Fig. 8 has more segmented regions than Fig. 7 with clear boundaries of objects. But this is not enough for automatic part identification and to decide the health of individual parts in the bogie.

A shape prior model for level set as a learning basis will focus on segmenting a particular bogie part and is useful in post processing recognition. Cremers [22] introduced the signed distance function for shape encoded level sets. To establish a unique relationship between its surrounding level set ϕ and a pre-defined shape model φ^{Shape} , it will be assumed that $\phi < 0$, inside φ^{Shape} , $\phi > 0$, outside φ^{Shape} and $|\phi| = 1$ everywhere else. There are many ways to define this signed distance function [30–32], out of which we use the most widely applied with constraints towards scaling, rotation and translational properties. In this work we propose to use initial contour ϕ and shape prior φ^{Shape} contour to compute level set area difference as in [33]:

$$d^2(\phi, \varphi^{Shape}) = \int_{\Theta} (H(\phi(x)) - H(\varphi^{Shape}(x)))^2 dx \quad (5)$$



Fig. 9. Frames of Coach 14 bogie 1 entry and exit.

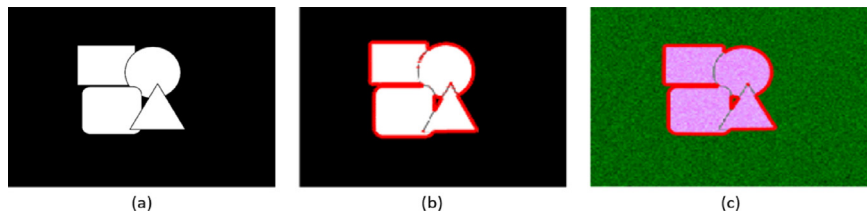


Fig. 10. (a) Simple multi shape model for testing the model. (b) Level set evolution with shape prior model (c) level set in the presence of noise.

The defined distance function is image size independent, nonnegative, symmetrical and satisfies triangle inequality. The challenging task is to feed the level set with only one shape prior model for all the 20,000 frames recorded for a train. As the train moves either to the left of the frame or to the right of the frame, the bogie has a lateral movement in only x-direction. However, the parts do not change their shape except in some cases where defects are present. Bogie part translation, scale and rotation invariance are the key to proposed shape invariance level sets. But for the case of rolling stock, the focus should be on translational alignment of shape term before application of level set functional due to the lateral movement of train in only one direction. Wide angle lens camera induces a small scale and rotation variance on the parts at different locations in the frame as shown in Fig. 9. In frame 15768, we can see the first part of rolling stock, i.e. wheel, entering the frame from right side. In the last frame i.e. 15981, the last part of rolling wheel exiting the frame from the right.

The shape invariance is preserved in most of the frames, except for minute changes in rotation due to shaking camera and medium scale changes due to fixed camera position. But a large translational change in the part shape model occurs as their location varies from frame to frame. This invariance level set function is given by

$$E^{Shape}(\phi) = d^2(\phi_0, \varphi^{Shape}) = \int_{\Theta} \left(-H(\phi_0(x)) + H(\varphi^{Shape}(s_\varphi x + t_\varphi)) \right)^2 dx \quad (6)$$

Here s_φ and t_φ are shape scale and translational values. Shape invariance is derived from the fractional evolving shape ϕ_0 , which is computed on same location and scale as Θ . Local energy minimization between $(\phi_0, \varphi^{Shape})$ maximizes the possibility of finding correct shape in the cluttered backgrounds. The affine transformations are defined by current shape ϕ_0 . The curve evolution expression is obtained by applying Euler-Lagrange equation on (6) as

$$\frac{\partial \phi_0}{\partial t} = 2\delta(\phi_0) \times (H(\varphi^{Shape}) - H(\phi_0)) \quad (7)$$

Where $\delta(\bullet)$ is delta function and t is artificial time step. Finally combining shape prior energy term in (6) and CV level set function in (2), we get the total energy function of the level set as

$$E^T = \zeta E^C + (1 - \zeta) E^{Shape} \quad (8)$$

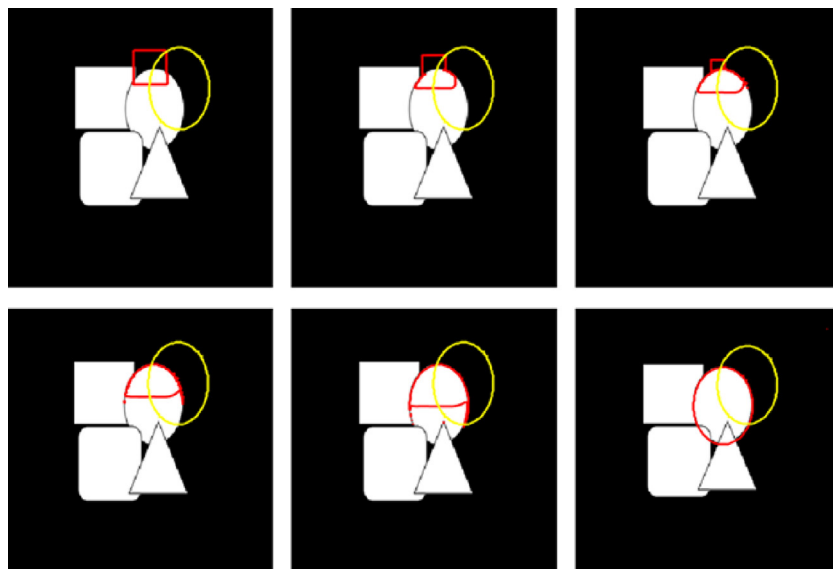


Fig. 11. Curve evolution from initial contour (red) with shape prior contour (yellow) for simulation with Eq. (9). (For interpretation of the references to colour in this figure legend, the reader is referred to the web version of this article.)

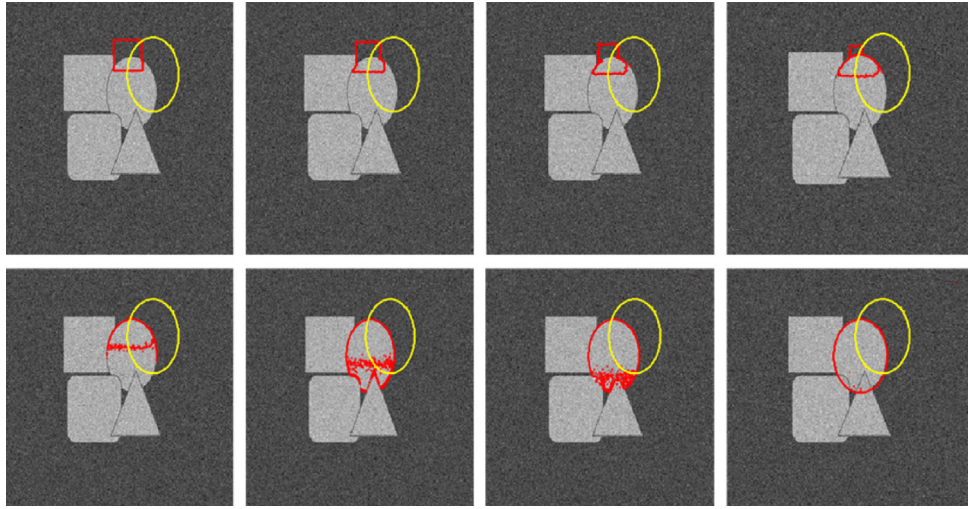


Fig. 12. Level set evolution on a speckle and noise added model image for testing the proposed model in Eq. (9).

Here ζ controls the effect of shape prior energy on the image energy. For single shape priors the energy functional used for algorithm development is derived from evolution equations in (3) and (7) is

$$\frac{\partial \phi}{\partial t} = \zeta \delta(\phi) \left[\lambda \left(\nabla \cdot \left(\frac{\nabla \phi}{|\nabla \phi|} \right) \right) - (I(x) - C^+)^2 + (I(x) - C^-)^2 \right] + 2(1 - \zeta) \times (H(\varphi^{Shape}) - H(\phi)) \quad (9)$$

Where C^+ and C^- are updated iteratively in each discrete time step using the expressions

$$C^+ = \frac{\int_{\Theta} I(H(\phi)) dx}{\int_{\Theta} (H(\phi)) dx} \quad (10)$$

$$C^- = \frac{\int_{\Theta} I \times (1 - H(\phi)) dx}{\int_{\Theta} (1 - H(\phi)) dx} \quad (11)$$

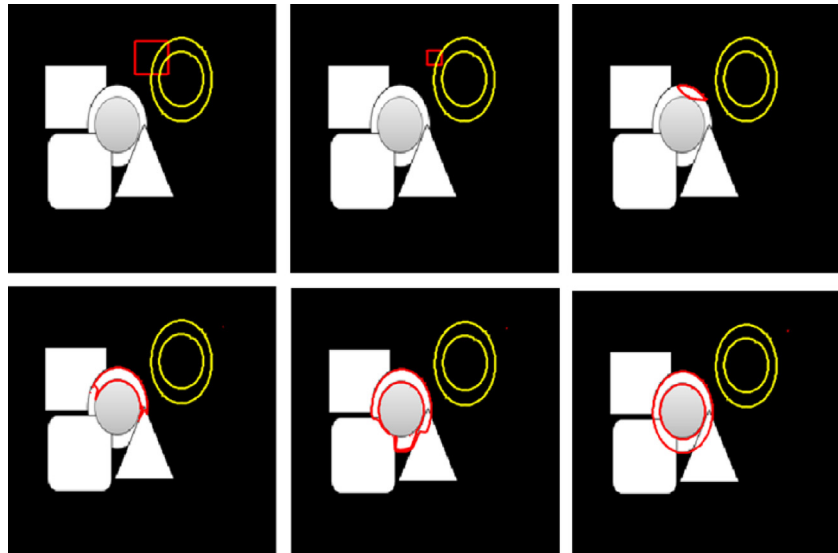


Fig. 13. Level set evolution with multiple edged shape displaying location invariance by perfectly aligning to the partially visible shape in the image under test.

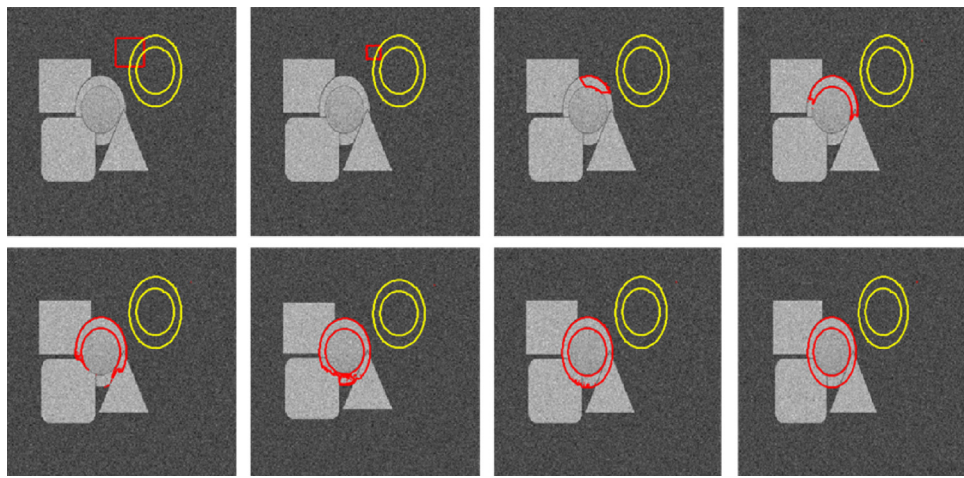


Fig. 14. Multi edged shape priors for object segmentation in the presence of speckle and salt & pepper noise variances of 0.7 each.

The model is first tested on a simple image having higher object density and overlapping shape objects as shown in Fig. 10(a). Fig. 10(b) and (c) show the final level set without shape prior term and the same in the presence of noise.

The evolving curve enclosed the whole image as a single object thereby losing the individual object shapes in the final segmentation. This is where shape priors models help identify overlapping and closely bound objects in an image. Figs. 11 and 12 show results of level set expression in Eq. (9). For this experimental image, the shape prior is a circle at a different location indicated in the figure by a yellow contour and the evolving level set is represented by a red contour.

By applying the proposed shaped level set model to video frames of rolling stock enables to check each item in an intelligent and nondestructive manner. But the rolling mechanical items have two walls binding the shape. Therefore the



Fig. 15. Train bogies recorded at the mentioned time steps.

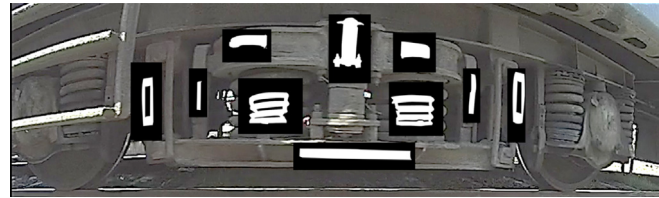


Fig. 16. Shape priors of bogie parts at their respective locations in the video frame.

shaped level set model has to successfully segment both inner and outer walls of the mechanical shapes. According to the theoretical analysis, the CV level sets are not edge triggered but region triggered models and therefore we test the model on double edge circular ring with and without noise components. [Figs. 13 and 14](#) gives the results of simulation where the shape prior model is not aligned with the image shape.

Shape prior is affine transformed based on translational parameter $t_\phi = [1, 0, 0; 0, 1, 0; x_\phi - x_\phi, y_\phi - y_\phi, 1]$ where (x_ϕ, y_ϕ) and (x_ϕ, y_ϕ) are shape centroid and object centroid. The object centroid is computed based on the location of initial contour, which usually is placed near to the object of interest. The translational parameter then calculates distance between the two centroids and tries to align the shape object with the region of interest object. For all the simulation shape term influence of $\zeta = 0.25$ and regularization influence of $\lambda = 0.02$ is used. All the simulations are timed to 100 iterations. The results display the usefulness of the model in applications with high noise object detection, hidden object detection and in our case tightly bound object extraction for analysis.

Application of the proposed and tested shape prior level set model on the real high-speed video data of the rolling stock to effectively separate parts for defect identification.

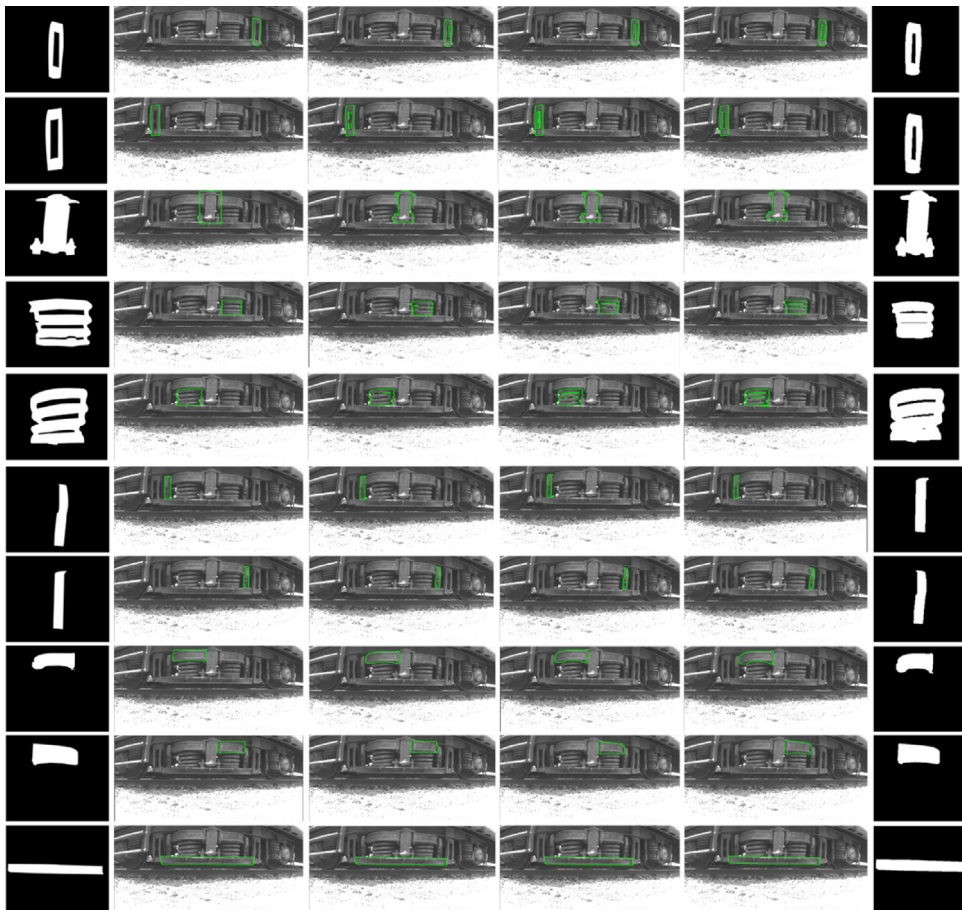


Fig. 17. The results of the proposed algorithm on a bogie frame. The first column represent shape priors of 10 bogie parts hand crafted from the frame. The next 4 columns represent the level set evolution process achieved by using the shape prior algorithm where the shape prior centroid is aligned with the bogie part centroid in the frame. The last column is shapes reconstructed from the level set obtained in the final iteration.

4. Experimentation and analysis

Video capture at lower frame rates of moving objects induces blurring and loss of object boundaries and regions. Normal cameras have a 30–60 fps capturing capacity, which is not useful for capturing rolling stock moving at around 30KMPH. To avoid blurring the frame rate should be at least twice the speed of objects in the image. This experimentation uses ISAW extreme sports action camera that can capture full HD at 30fps, 60fps, 120fps and 240fps with wireless transmissions up to a distance of 10 m. To record an entire bogie, the camera is set in 240fps, with 16:9 unscaled aspect ratio and 152° field of view giving 853 × 480 sized video frames. Bogie recording at four different time steps at 7.00AM, 12PM, 5PM and 7PM of 10 different trains is the database used for testing the proposed method. Fig. 15 shows frames of 5 train bogies at the cited time intervals.

Fig. 15(d) and (e) are at same time but with two different focus lighting used by Indian Railways, i.e. Fig. 15(d) is bogie under white focus light and Fig. 15(e) is under yellow light. The first obstacle is to normalize the contrast of all recordings due to uneven brightness distribution during recording. As mentioned in our previous work, we used virtual contrast enhancement for the video frame as a preprocessing. More information can be found at [34]; [35].

The initial contour and shape model powered level set is set on the contrast improved video frames. For experimentation we focus on the following shape priors embedded on the original video frame as shown in Fig. 16.

The performance estimation of the proposed level set on train video frames is quantitatively and qualitatively presented in the following sections. We present the results in five parts. Part 1, provides bogie parts segmentation with the shape prior located at the same location as the part in the video frame. The second part gives shape invariance concept of the method irrespective of location of the shape prior. Part 3 of the results evaluates the performance of the algorithm for parts masked by some other parts during movement. The fourth part tries to use the same algorithm to identify defects and same non-defective shape priors introduced into the bogie parts. Finally, part 5 presents a comparison with other popular shape prior algorithms like [20,36,37] with the proposed method.

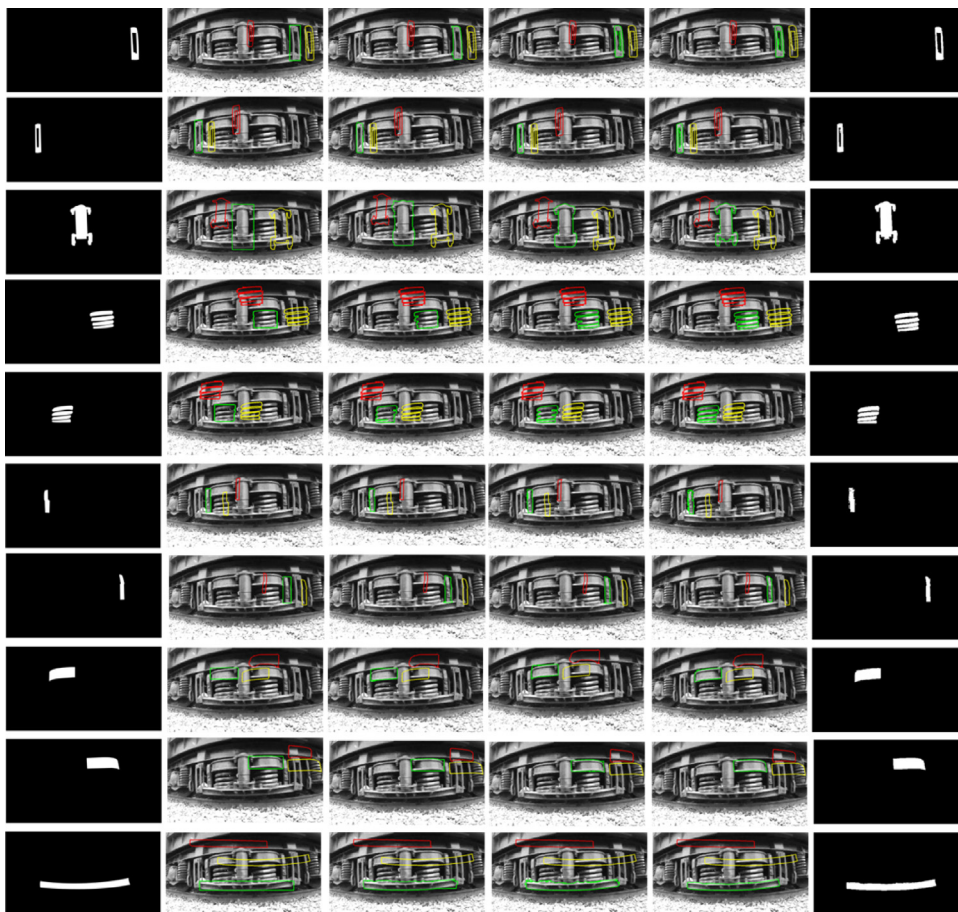


Fig. 18. Experiment 2 of the proposed shape prior model on a bogie frame of a different train captured under low natural light at 7:00 AM from Fig. 15(a). The first column represents shape priors of 10 bogie parts hand crafted from the frame. The next 4 columns represent the level set evolution process and the last column gives reconstructed parts from the level set obtained in the final iteration.

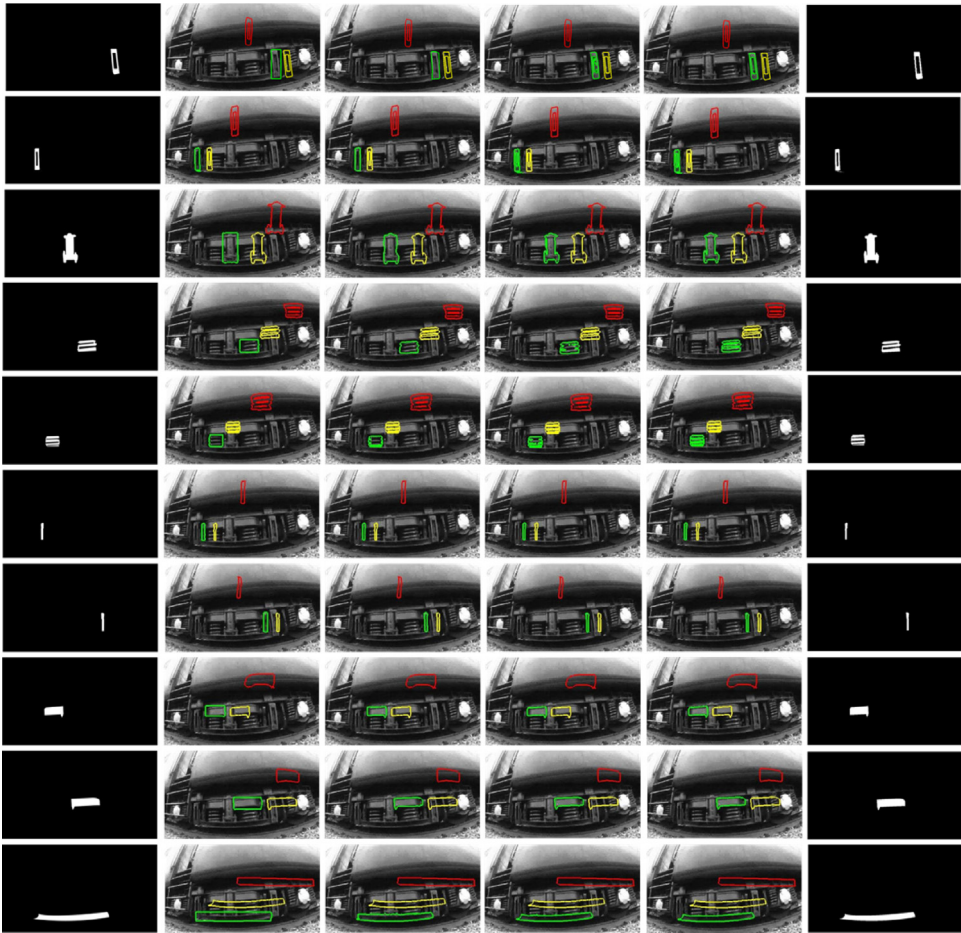


Fig. 19. Experiment 3 of the proposed shape prior model on a bogie frame of a different train captured under low natural light at 5:00 PM from Fig. 15(c). The first column represent shape priors of 10 bogie parts hand crafted from the frame. The next 4 columns represent the level set evolution process and the last column gives shapes reconstructed on the last level set iteration.

The previous section detailed the results on synthetic images with and without noise refer Figs. 11–14. Experiment 1 and 2 applies the algorithm on video frames 15(a) and (b) of two different trains with the same bogie configuration. Fig. 17 shows the curve evolution on video frame in Fig. 15(b). The same train bogie is used to make the shape priors. For experimentation the value of λ is 0.02 and ζ is 0.13. But the parametric values are increased slightly: ($\lambda = 0.2$ and $\zeta = 0.32$) to accommodate complex shapes like springs and the central holding rod (rows 3–5 in Fig. 17). Visual analysis of the reconstructed shapes such as springs shown in rows 4 and 5, projects a merger performance of the algorithm in detecting fine region between last two rings in the spring. However, the overall shape and region of the spring is preserved to perfection.

In the next experiment we test the robustness of the algorithm on a set of frames from different train bogie with the configuration similar to shown in Fig. 15(a). The trouble in using the same shape priors emulated the contour energy due to scale difference between shape model and actual object of the interest in the frame. Scale adjustment parameters s_φ helps in correcting the shape changes by computing the unscaled shape prior on a frame in the first 70 iterations and subtracting this partial result from the unscaled shape prior model. If this difference is positive, the scale of the shape prior reduces by s_φ and if it is negative it increases by s_φ . The second experiment uses this for self-correcting the scale changes and the resulting part segments are shown in Fig. 18.

Only difficulty being the precise control of combination of image forces and shape prior forces for complex shapes such as springs and the central holding rod. For springs the shape term ζ is 0.39 and for central rod it is 0.42. For all other shapes in Fig. 18 ζ is 0.16. The average iterations per frame in experiment 2 is 56. The number of iterations is directly proportional to object size and number of non-planer curves in the object. The minimum iteration count is 38 for objects segmented in the second half of Fig. 18. The maximum number of iterations is 89 for the center binding rod, the row 3 object in Fig. 18.

Color coding in Figs. 18–20 is helpful in identifying the original shape prior and translational shape prior. The original shape prior model for all bogies on all trains having same bogie configuration is colored in red. Yellow color is given to the shape prior which is scaled, rotated and shifted according to the object shape extracted from the first-run. Green is the color code of the evolving contour on the video frame.

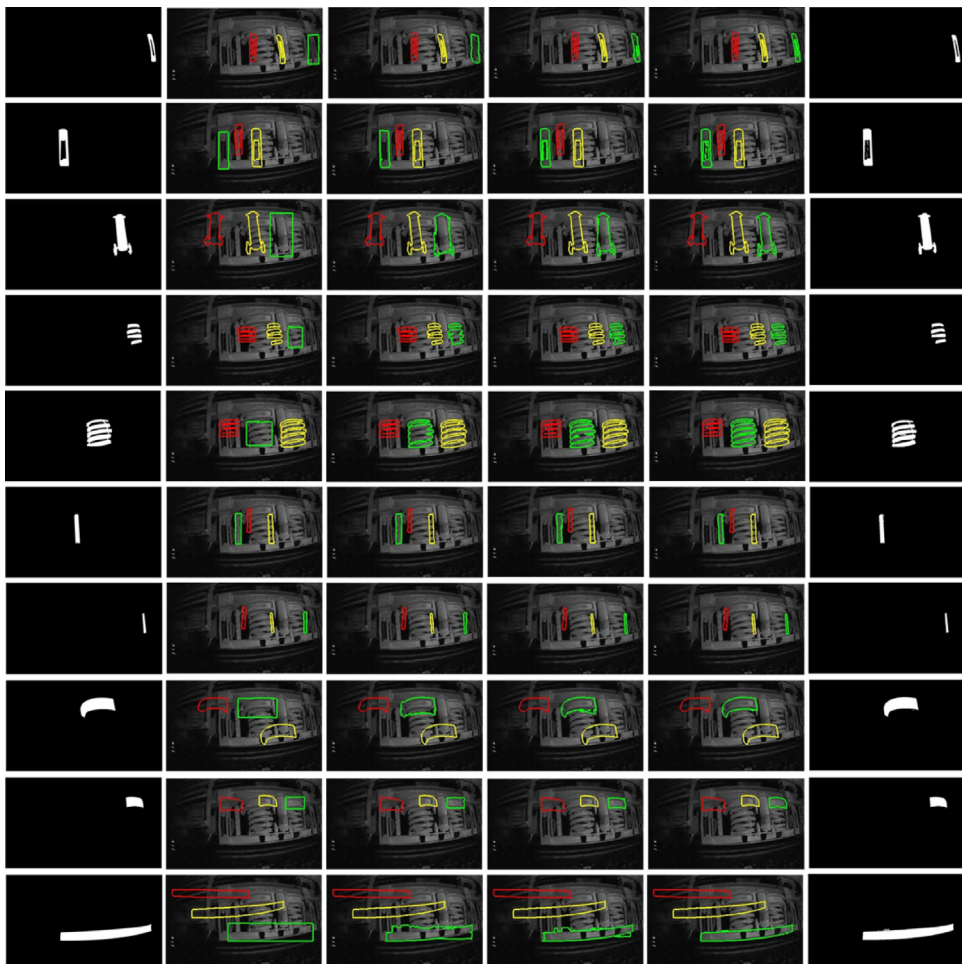


Fig. 20. Experiment 4 of the proposed shape prior model on a bogie frame of a different train captured under low natural light at 7:00 PM from Fig. 15(d). The first column represent shape priors of 10 bogie parts hand crafted from the frame. The next 4 columns represent the level set evolution process and the last column presents shapes reconstructed from the level set obtained in the final iteration.

Fig. 19, gives the results of algorithm on frames in Fig. 15(c). This is challenging as the video frame is differently aligned to the shape prior objects. As the train bogie configuration is unchanged, we use the same shape priors for segmentation on Fig. 15(c). Scaling and translation were dominant on this frame whereas rotation is hardly used except for a few parts. The adjustments to shape alignment made execution longer for the first frame. From the second frame onwards the result of the previous frame is used as a shape prior with minimum translations. Fig. 20 shows the algorithm performance during night rolling examination, i.e. the video captured under white light. Yellow light rolling examination requires more trials because of poor image quality during capture thus making us postpone this study from this work.

The shape priors were introduced at first into computer vision to segment masked or occluded objects in a video frame. The next experiment tests the proposed algorithm on frames of occluded parts and their correct shape extraction. Capturing real time bogie frames having valuable information marked by occult objects is impossible. The main occlusion, partly though comes from the climbing steps on each side of the coach as can be seen in Fig. 9. Experiment 3 tests this ability of the proposed method for detecting partly hidden parts during rolling stock examination.

Carefully controlling the shape influence term ζ is the key for this experiment to extract correct part shapes. Too much or too little of ζ will result in unwanted segments. The value of the parameter ζ depends on the amount of shape occluded in the frame. Iterative testing has enabled us to create an area based expression given by the ratio of segmented object in the first-run and shape prior object

$$\zeta = \frac{(A^{SP} - A^S)^2}{(A^{SP})^2 + (A^S)^2} \quad (12)$$

where A^{SP} is area of shape prior object and A^S is area of the object segment from the first-run. Experiment 3 uses frames from the left binding lever which is occulted by the steps as shown in Fig. 21. The occulted object lever is being segmented



Fig. 21. Occluded holding screw from the climbing ladder.

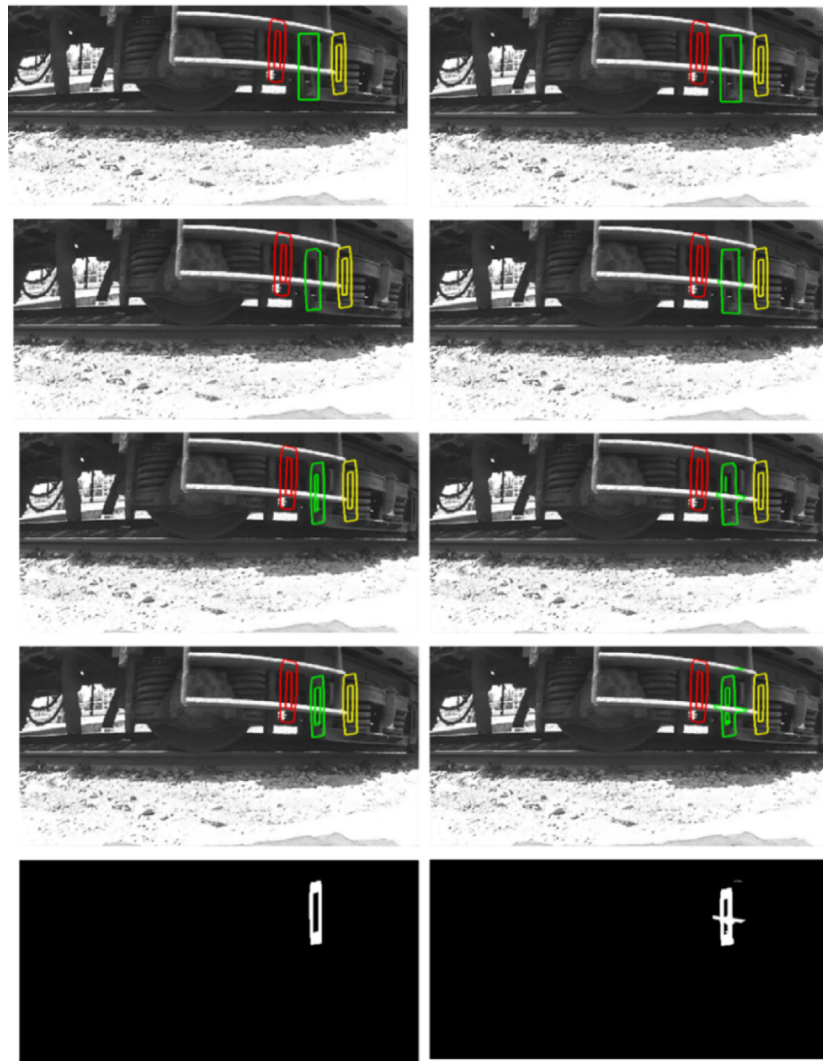


Fig. 22. (a) Result of occluded object segmentation with 0.32 shape prior energy term and 0.68 image term. (b) segmentation result on the same frame with shape of 0.28.

with the same shape prior used for segmentation without occlusion. The value of ζ , for the job from equation 12, is 0.32. The variational contour movement under the shape term influence produces a segmentation result as shown in Fig. 22. Maximum iteration count is 67 with a virtual time step of 0.5 per iteration. Any value of ζ lower than 0.32, the movement gets disrupted due to external forces exerted by other objects in the image frame. The major obstacle in extracting correct part shapes is coming from object packing density of the bogie parts. Object packing density marks the closeness of object

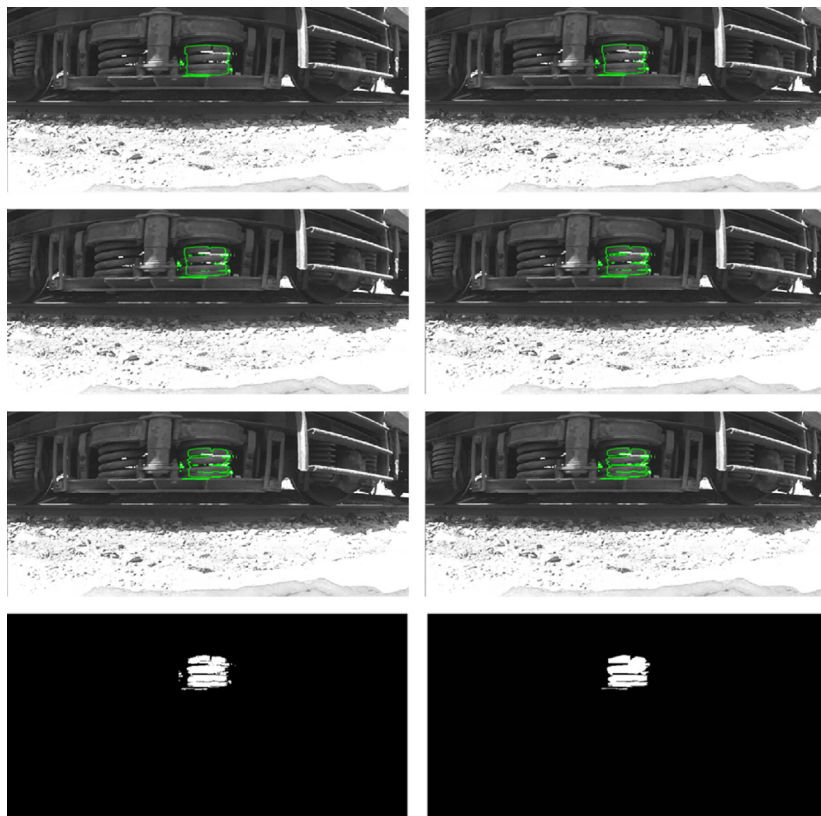


Fig. 23. Defective part segmentation with non-defective shape prior with increased image energy term and decreased shape prior term. Images show curve evolution and with the last row showing binary segment of the defective spring and its morphological binary with removed over segmented portions.

regions overlapping into one another. Hence we show the shape prior segmentation with precise control of shape energy term gives good shape segments of occluded parts in video frames.

Fig. 22(a) and (b) compares the influence of shape prior energy on the level set evolution. By precisely controlling the ζ parameter, better segmentation of partly hidden parts in a bogie can be accomplished with the proposed algorithm.

The train rolling examination finds defective parts in the bogie which can cause interruption to train movement and further become a cause for an accident. To help manual system of defect identification into an intelligent nondestructive testing model is the final goal of this work. Also to formulate an expert system that can identify and report rolling defects online in real time for quick action. The next experiment relates to identifying defective parts during transit. As we could not capture defects in real time, we simulated them in virtually.

A bogie secondary suspension spring is broken in one of its rings as shown in Fig. 23. The algorithm uses the same shape prior of spring used earlier to extract spring from the bogie video. For this experiment the shape prior term parameter decreases to a level where the level set does not explode or implode on the image object. The shape parameter is taken as 0.18, which makes the level set energy flow on the image instead of the model. Fig. 23 validates the process of curve evolution. The last row in Fig. 23 is the binary image with clear defect representation and its morphological binary with removed over segmented portions. Since it is difficult to predict the exact defect type, the proposed method is made to identify defects with non-defective shape prior terms. Fig. 24 shows a two location broken spring of the same spring suspension in the same bogie. The figure shows curve evolution and binary images in the last row giving encouraging results of the proposed method towards defect identification in bogie parts.

Experiment 5 tests the robustness of the proposed algorithm against the popular level set models like, Chan Vese, Geodesic and Samuels. Same shape prior is used for all algorithms with 0.32 shape term parameter. The difference can be observed in Fig. 25. The proposed method which used Cramer's level set model with translational and rotational alignments based on single video frame outperforms the other three level set models. All models used same parameters during execution. The number of iterations for the proposed method for spring is 74 which is 25% lower than the other three models. The next step is building an expert system from these segmented parts for classification of parts and identifying defects.

An evaluation of the algorithm with respect to segmentation accuracy is performed. For evaluation we compute two parameters. One being the Euclidian distance between segmented result from the algorithm to the ground truth. Second gives the ratio of segmented part area from algorithm to ground truth area. If the distance and area ratio are small the

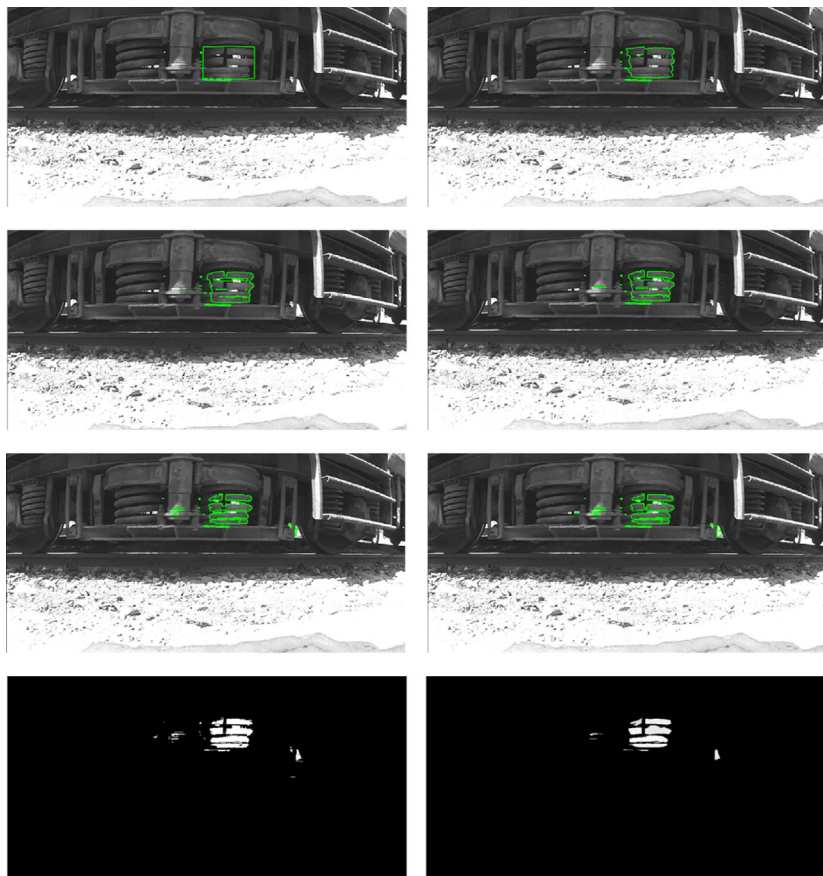


Fig. 24. Multiple defects segmentation with non-defective shape prior and last row producing binary equivalents of the defective spring.

segmentation result from the proposed algorithm is worthy and can be used for further classification. The proposed method for rolling stock segmentation recorded lower values for all the parts segmented in comparison to other three level set models used in this work.

Experimentation of the shape prior invariance level set algorithm for rolling stock video segmentation is carried on an intel core i7 processor with 8GB Ram and MATLAB 15 software. The proposed method is faster on simulation time compared with other three models. The algorithms processing speed for defect identification coupled with a pattern classifier will help in faster repairs during inter station train stops. For a single bogie capture, the high-speed camera hit 200 frames and for a single coach with two bogies it captures 400 frames. When simulated for a particular train in Fig. 15(b) we could generate a time gap of 12.2 min for a train with 10 coaches and 20 bogies. This time can be trimmed by incorporating high-speed cloud based servers for processing. By using a 48 node super computer the time gap between input and output was cut down to 3.89 min. With extensive testing and evaluation of the proposed shape invariance level set model can be incorporated into railway service for intelligent system monitoring and maintenance.

5. Conclusion

This paper applies computer vision to railway engineering systems for failure checking during rolling stock examination. A shape, position and brightness invariant level set model is proposed in this work to segment rolling parts of a bogie from high-speed video of a moving train. A single shape prior model powered level sets helps in segmenting bogie parts on multiple trains under various lighting conditions. Shape prior term distributed in lower dimension subspace provides more accurate estimate of the targeted shapes with similar pixel arrangement and high packing density. This data driven level sets in computer vision provide better rolling part segmentation for defect segmentation with non-defective shape priors. We further try to save trains by developing algorithms to classify rolling defective parts at a faster rate for quick maintenance by lessening the computation time.

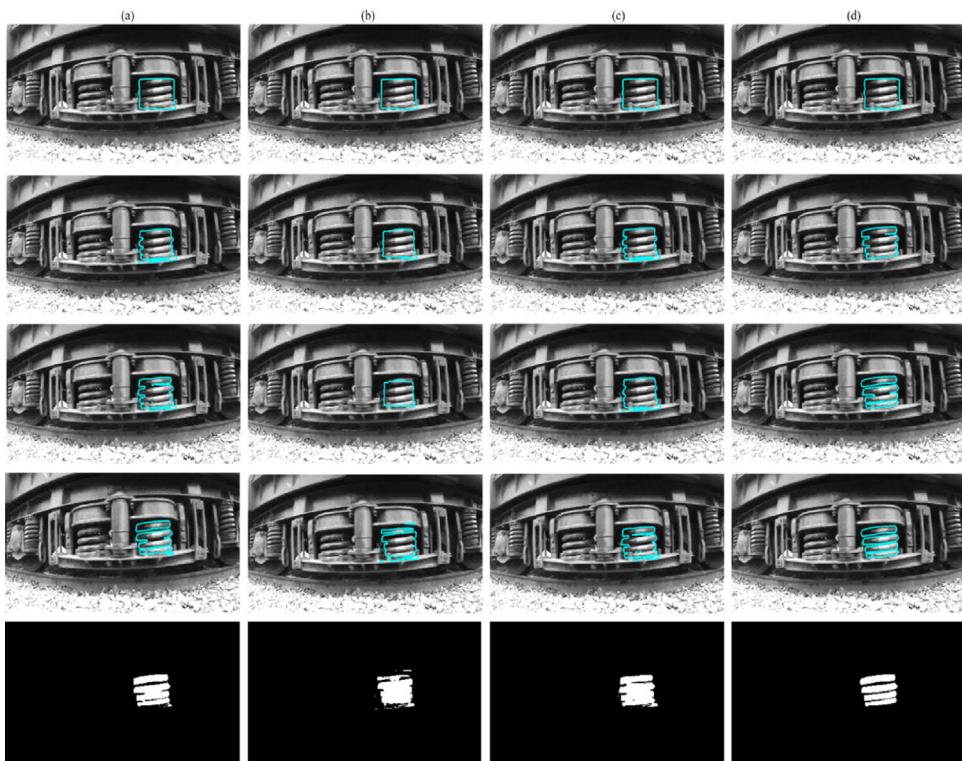


Fig. 25. Column (a) Chan Vese Model [20] with Shape prior and its final segmented rolling part. (b) Geodesic Level set [36] evolution (c) Samuels level set [37] evolution and final segmented output.

References

- [1] <http://www.intlrailsafety.com/capetown/3.024.amitabh.doc>.
- [2] T. Ashwi, S. Ashok, Automation of rolling stock examination, Proceeding of IEEE International Conference on Advanced Communication Control and Computing Technologies (ICACCT) (2014) 260–263.
- [3] P.V.V. Kishore, C.R. Prasad, Train rolling stock segmentation with morphological differential gradient active contours, Proceedings in 2015 IEEE International Conference on Advances in Computing, Communications and Informatics (ICACCI) (2015) 10–13, 1174–1178.
- [4] Kosmopoulos Dimitrios, Theodora Varvarigou, Automated inspection of gaps on the automobile production line through stereo vision and specular reflection, *Comput. Ind.* 46.1 (2001) 49–63.
- [5] Vicente Milanés, David F. Llorca, Jorge Villagrá, Joshué Pérez, Carlos Fernández, Ignacio Parra, Carlos González, Miguel A. Sotelo, Intelligent automatic overtaking system using vision for vehicle detection, *Expert Syst. Appl.* 39 (3(15)) (2012) 3362–3373.
- [6] Habib Fathi, Fei Dai, Manolis Lourakis, Automated as-built 3D reconstruction of civil infrastructure using computer vision: achievements, opportunities, and challenges, *Adv. Eng. Inf.* 29 (2) (2015) 149–161.
- [7] Hang Zhang, Daoliang Li, Applications of computer vision techniques to cotton foreign matter inspection: a review, *Comput. Electron. Agric.* 109 (2014) 59–70.
- [8] Yuxiang Yang, Zheng-Jun Zha, Mingyu Gao, Zhiwei He, A robust vision inspection system for detecting surface defects of film capacitors, *Signal Process.* 124 (2016) 54–62.
- [9] Wang Lingzhi, Xu Yugong, Zhang Jiadong, Importance analysis on components in railway rolling stock based on fuzzy weighted logarithmic least square method, *Intelligent Computing and Intelligent Systems (ICIS), 2010 IEEE International Conference on* 1 (2010) 175–179.
- [10] A. Mor-Yaroslavtsev, A. Levchenkov, Rolling stock location data analysis using an immune algorithm on an intelligent embedded device, *Telecommunications Forum (TELFOR)* 22 (24 (19th)) (2011) 1554–1557.
- [11] Won Young Yun, Young Jin Han, Goeun Park, Optimal preventive maintenance interval and spare parts number in a rolling stock system, *Quality, Reliability, Risk, Maintenance, and Safety Engineering (ICQR2MSE), 2012 International Conference on* 15 (18) (2012) 380–384.
- [12] R.W. Lewis, S. Maddison, E.J.C. Stewart, An extensible framework architecture for wireless condition monitoring applications for railway rolling stock, *Railway Condition Monitoring (RCM 2014), 6th IET Conference on* 17 (18) (2014) 1–6.
- [13] J.-B. Boullie, M. Brun, A new rolling stock architecture using safety computers and networks, in: *Dependable Systems and Networks, 2000. DSN 2000, Proceedings International Conference on* (2000) 157–162.
- [14] H. Sato, H. Nishii, S. Adachi, Automatic thickness measuring system by image analysis for brake shoes of traveling rolling stock, *Kawasaki Steel Tech. Rep.* 27 (1992) 77–83.
- [15] H. Kim, W.-Y. Kim, Automated thickness measuring system for brake shoe of rolling stock, *Proceedings of 9th IEEE Workshop Applications of Computer Vision* (2009) 1–6.
- [16] Hwang Jungwon, Hu-Young Park, Whoi-Yul Kim, Thickness measuring method by image processing for lining-type brake of rolling stock, *Network Infrastructure and Digital Content, 2010, 2nd IEEE International Conference on* 24 (26) (2010) 284–286.
- [17] Stanley Osher, James A. Sethian, Fronts propagating with curvature-dependent speed: algorithms based on Hamilton-Jacobi formulations, *J. Comput. Phys.* 79 (1) (1988) 12–49.
- [18] Ravi Malladi, James A. Sethian, Baba C. Vemuri, Shape modeling with front propagation: a level set approach, *IEEE Trans. Pattern Anal. Mach. Intell.* 17 (2) (1995) 158–175.

- [19] Vicent Caselles, Ron Kimmel, Guillermo Sapiro, Geodesic active contours, *Int. J. Comput. Vis.* 22 (1) (1997) 61–79.
- [20] Tony F. Chan, Luminita A. Vese, Active contours without edges, *IEEE Trans. Image Process.* 10 (2) (2001) 266–277.
- [21] Thomas Brox, Joachim Weickert, A TV flow based local scale measure for texture discrimination, in: *European Conference on Computer Vision*, Springer, Berlin, Heidelberg, 2004.
- [22] Daniel Cremers, Stanley J. Osher, Stefano Soatto, Kernel density estimation and intrinsic alignment for shape priors in level set segmentation, *Int. J. Comput. Vis.* 69 (3) (2006) 335–351.
- [23] M. Rousson, D. Cremers, Efficient kernel density estimation of shape and intensity priors for level set segmentation, *Intl. Conf. on Medical Image Computing and Comp. Ass. Intervention (MICCAI)* (2005) 757–764.
- [24] A. Tsai, A. Yezzi, W. Wells, C. Tempany, D. Tucker, A. Fan, E. Grimson, A. Willsky, Model-based curve evalution technique for image segmentation, in: *Comp. Vision Patt. Recog. Kauai, Hawaii*, 2001, pp. 463–468.
- [25] Daniel Cremers, Sochen Nir, Christoph Schnörr, A multiphase dynamic labeling model for variational recognition-driven image segmentation, *Int. J. Comput. Vis.* 66 (1) (2006) 67–81.
- [26] Yunmei Chen, et al., Using prior shapes in geometric active contours in a variational framework, *Int. J. Comput. Vis.* 50 (3) (2002) 315–328.
- [27] M. Rousson, N. Paragios, Shape priors for level set representation, in: A. Heyden, et al. (Eds.), *Europ. Conf. on Comp. Vis.*, vol. 2351 of *Lect. Not. Comp. Sci.*, Springer, 2002, pp. 78–92.
- [28] Anthony J. Yezzi, Stefano Soatto, Deformation: deforming motion, shape average and the joint registration and approximation of structures in images, *Int. J. Comput. Vis.* 53 (2) (2003) 153–167.
- [29] P.V.V. Kishore, A.S.C.S. Sastry, Zia Ur Rahman, Double technique for improving ultrasound medical images, *J. Med. Imaging Health Inf.* 6 (3) (2016) 667–675.
- [30] M. Sussman, P. Smereka, S. Osher, A level set approach for computing solutions to incompressible two-phase flow, *J. Comput. Phys.* 114 (1) (1994) 146–159.
- [31] Laadhari Aymen, Pierre Saramito, Chaouqi Misbah, An adaptive finite element method for the modeling of the equilibrium of red blood cells, *Int. J. Numer. Methods Fluids* 80 (7) (2016) 397–428.
- [32] Daniel Kraft, Self-consistent gradient flow for shape optimization, *Optim. Methods Softw.* (2016) 1–13.
- [33] Charpiat Guillaume, Olivier Faugeras, Renaud Keriven, Approximations of shape metrics and application to shape warping and empirical shape statistics, *Found. Comput. Math.* 5 (1) (2005) 1–58.
- [34] B.T.P. Madhav, P. Pardhasaradhi, R.K.N.R. Manepalli, P.V.V. Kishore, V.G.K.M. Pisipati, Image enhancement using virtual contrast image fusion on Fe3O4 and ZnO nanodispersed decyloxy benzoic acid, *Liq. Cryst.* 42 (9) (2015) 1329–1336.
- [35] P.V.V. Kishore, Ch. Raghava Prasad, Shape prior active contours for computerized vision based train rolling stock parts segmentation, *Int. Rev. Comput. Softw. (I.R.E.C.O.S.)* 10 (12) (2015).
- [36] Bin Wang, et al., A level set method with shape priors by using locality preserving projections, *Neurocomputing* 170 (2015) 188–200.
- [37] Wang Junqiu, Yasushi Yagi, Shape prior's extraction and application for geodesic distance transforms in images and videos, *Pattern Recognit. Lett.* 34 (12) (2013) 1386–1393.